A Physical Compact MOSFET Mobility Model Including Accurate Calculation of Saturation Surface Potential.

J. Benson*, N. V. D'Halleweyn**, K. Mistry*, and W. Redman-White***

* Department of Electronics and Computer Science,
University of Southampton, Southampton, U.K., jb3@ecs.soton.ac.uk
** now with Arnold and Siedsma, Antwerp, Belgium.
*** Philips Semiconductors, San Jose, U.S.A.

ABSTRACT

We describe a vertical field electron mobility model that has been implemented in a SOI MOSFET surface potential based compact model. The main scattering mechanisms - surface roughness, phonon, and Coulomb scattering - are included.

All scattering terms have been retained when calculating the drain saturation surface potential ψ_{sLsat}. This yields a quartic expression in ψ_{sLsat}. Taking the exact quartic solution results in numerical instabilities in ψ_{sLsat} under some conditions, which cannot be corrected using numerical limiting. Instead, a method has been devised in which the quartic is approximated by a stable quadratic expression. The accuracy of the approximate solution is very high, with deviations from the exact solution of no more than a few mV.

Keywords: MOSFET, compact modelling, surface potential, mobility, quartic.

1 INTRODUCTION

Inversion layer mobility has an important influence on the behaviour of MOSFET devices, and compact models need to accurately model the variation of the mobility with electric field. Until recently, it was commonplace for circuit simuators to rely on the classic empirical relation [1], [2]

$$\mu_{xeff} = \frac{\mu_0}{1 + \alpha_\theta E_{xeff}} \tag{1}$$

where μ_0 is the bulk mobility, μ_{xeff} is the vertical field degraded effective mobility, E_{xeff} is the effective vertical electric field, and α_θ is a fitting constant. Using this relation yields simple, tractable expressions for the drain current, but at the cost of reduced physical accuracy. Extensive parameter optimisation, often accompanied by non-physical scaling of parameters with channel length, is normally required to match experimental results.

Although models have been devised which incorporate the main physical mobility scattering mechanisms [3], [4], it was not until quite recently that these started to appear in compact models [5],[6]. One reason for this is that they yield more complex mathematical expressions. In particular, problems can arise when calculating the drain saturation surface potential ψ_{sLsat}. In surface potential-based models, ψ_{sLsat} is a very important quantity, since it determines the point of transition between the linear and saturation operating regimes. In order to avoid the complexity of high-degree polynomial expressions, it is necessary to either ignore or simplify some of the scattering terms, or else neglect the effects of the vertical field on ψ_{sLsat}. Both approaches introduce an undesirable error.

2 MODELLING OF SCATTERING MECHANISMS

This paper describes a MOSFET vertical field mobility model that has been implemented in a surface potential based compact model, STAG [7]. The main scattering mechanisms are accounted for using the following expression:

$$\mu_{xeff} = \frac{\mu_0}{1 + G_{ph} + G_{sr} + G_{cou}} = \frac{\mu_0}{G_v} \tag{2}$$

where G_{ph}, G_{sr}, and G_{cou} are the contributions due to phonon, surface roughness, and Coulomb scattering respectively. In the following sections, α is used to denote a model parameter.

2.1 Phonon Scattering

The generally accepted dependence of phonon scattering on vertical field in a MOS inversion layer is given by [4]

$$G_{ph} = \alpha_{ph} E_{xeff}^{1/3} \tag{3}$$

A standard equation for E_{xeff} is used to determine the functional dependence of G_{ph} on the device surface potential

$$E_{xeff} = \frac{(f_b q_b + f_c q_c)}{\epsilon_{Si}} \tag{4}$$

fb and fc have been ascribed functional dependencies [8], but are more usually set to constant values of 1

and 0.5 respectively. q_b and q_c are the body and channel charge densities, and are modelled by standard surface potential expressions [1], [2]. Once G_{ph} has been expressed in terms of the surface potential, it is necessary to perform a Taylor expansion to obtain an integer power expression.

2.2 Surface Roughness Scattering

Surface roughness scattering starts to dominate over phonon scattering at higher gate voltages. While the power dependence of this scattering mechanism is somewhat influenced by the interface quality and gate material [9], the most commonly used expression for electron scattering at the oxide interface is

$$G_{sr} = \alpha_{sr} E_{xeff}^2 \tag{5}$$

2.3 Coulomb Scattering

This scattering contribution is most dominant close to the threshold voltage, since scattering due to ionised impuries is greatly reduced by the screening of the inversion layer at higher gate voltages. It has been found empirically that the magnitude of the scattering term is inversely proportional to the channel charge density [4]. In order to obtain a more numerically stable expression, the approach taken by Villa et al [10] was adopted. Since the emphasis is on deriving an accurate expression around threshold, at low inversion charge densities, a non-degenerate version of (10) in [10] was derived. This then leads to an expression of the form:

$$G_{cou} = \alpha_{cou} N_A \left(\frac{q_{s0}}{q_{s0} + q_c} \right)^2 \tag{6}$$

where N_A is the doping concentration, and q_{s0} is some characteristic charge density associated with the screening of the inversion layer.

3 CALCULATION OF SATURATION SURFACE POTENTIAL

The STAG model uses an expression for the channel current I_{CH} of the form:

$$I_{CH} = \frac{W}{L} \mu_{eff} C_{ox} \left[f(\psi_{sL}) - f(\psi_{s0}) \right] \tag{7}$$

where W, L, C_{ox}, have their usual meanings, ψ_{s0} and ψ_{sL} are the surface potentials at the source and drain ends of the channel, and μ_{eff} is the total effective mobility, given as

$$\mu_{eff} = \frac{\mu_0}{G_v + \frac{\mu_0 (\psi_{sL} - \psi_{s0}))}{v_{sat} L}} \tag{8}$$

Note that μ_{eff} differs from μ_{xeff} in that it also includes a term accounting for the effect of velocity saturation (v_{sat} is the carrier saturation velocity).

We define ψ_{sLsat} as the drain surface potential at which the channel current turns over (reaches saturation). Therefore, $\psi_{sL} = \psi_{sLsat}$ when the following condition is met:

$$\frac{\partial I_{CH}}{\partial \psi_{sL}} = 0 \tag{9}$$

If ψ_{sLsat} is over-estimated, it can result in a non-physical rollover of the channel current [11]. It is therefore important to ensure that ψ_{sLsat} is calculated as accurately as possible.

If we use (2) - (8) and convert to a surface potential equation using standard expressions for q_b and q_c, we can apply (9) to obtain a quartic equation in ψ_{sLsat}:

$$A\psi_{sLsat}^4 + B\psi_{sLsat}^3 + C\psi_{sLsat}^2 + D\psi_{sLsat} + E = 0 \tag{10}$$

Following the same procedure as in [11], we apply the following substitution

$$\psi_{sLsat} = \psi_{s0} + \frac{\Psi}{S} \tag{11}$$

In the limit of no velocity saturation, $S = 1$, whilst in the limit of excessive velocity saturation, $S \to \infty$. The definitions of S and Ψ are given in [7]. By substituting (11) into (10), we obtain a quartic expression in S:

$$aS^4 + bS^3 + cS^2 + dS + e = 0 \tag{12}$$

It is possible to solve (12) directly, but the roots can exhibit numerical discontinuities. For this reason a technique was developed to make the equation more stable. We begin by applying another substitution to give a second degree polynomial:

$$S = \left(z^{\frac{1}{2}} - \frac{b}{4a} \right) \tag{13}$$

By substituting (13) into (12), we obtain the following expression:

$$az^2 + \left(c - \frac{3b^2}{8a} \right) z + \left(\frac{b^3}{8a^2} + d - \frac{bc}{2a} \right) z^{\frac{1}{2}} + \left(\frac{b^2 c}{16a^2} - \frac{3b^4}{256a^3} - \frac{bd}{4a} + e \right) = 0 \tag{14}$$

Note that the inclusion of the second term on the right-hand side of (13) causes the $z^{3/2}$ terms to cancel

out. We are now left with just one term containing a fractional power of z. By applying a second-order Taylor expansion to this $z^{1/2}$ term, about some value z_0, we obtain a quadratic equation in z.

$$Pz^2 + Qz + R = 0 \tag{15}$$

By solving (15), and then applying (13) and (11) in reverse, we obtain ψ_{sLsat}.

3.1 Derivation of z_0

In order to ensure that our approximate value of ψ_{sLsat} closely matches the exact quartic solution, it is important to carefully determine the value of the Taylor expansion variable z_0. It has been found that merely using a constant value for z_0 does not provide sufficient accuracy under all conditions. Instead, a technique has been developed to dynamically vary z_0 in a physically appropriate way.

We begin by setting the vertical mobility contributions to be independent of ψ_{sL}, which simplifies the differentiation in (9)). The simplest approach is to neglect G_{ph}, G_{sr}, and G_{cou}, such that $G_v = 1$. Thus the only contribution to mobility degradation now comes from the velocity saturation term (see (8)).

Having done this, we now proceed as before, using the condition in (9) to define ψ_{sLsat}. Due to the greatly simplified nature of the mobility expression, we obtain a quadratic equation in ψ_{sLsat}:

$$l_0\psi_{sLsat}^2 + m_0\psi_{sLsat} + n_0 = 0 \tag{16}$$

By solving (16), and then using (11) and (13), we obtain z_0. When solving the quadratic, it is necessary to ensure that the correct root is selected, by remembering that S cannot physically fall below 1.

The main benefit of calculating z_0 in this way is that it eliminates scaling problems. Since S (which as discussed earlier represents the degree of velocity saturation) and hence z_0 vary with channel length, any constant value chosen for z_0 is unlikely be valid for both long and short-channel devices. Since channel length dependence is only present in the velocity saturation term, we can factor out its influence by using the above technique. Additional accuracy can be achieved by setting G_{ph}, G_{sr}, and G_{cou} so that G_v has a non-zero value, whilst keeping them functionally independent of ψ_{sL}.

4 MATHEMATICAL EVALUATION

There are two main considerations when evaluating the new mathematical model. The first is whether the approximated solution closely matches the exact solution, and the second is whether it provides improved numerical stability. As can be seen from Figure 1, deviation from the exact solution is typically a few mV at most, and even this worst case only occurs for excessive gate voltages. This allows a small correction factor to be applied to the approximate solution of ψ_{sLsat}, to ensure that it is always slightly below the exact solution, and thus avoid channel current rollover.

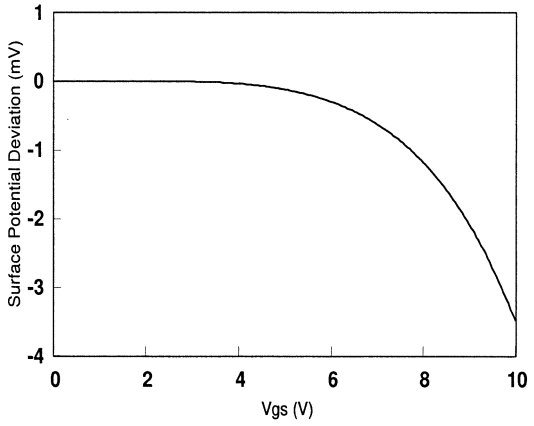

Figure 1: Deviation of approximate solution for ψ_{sLsat} from exact quartic solution.

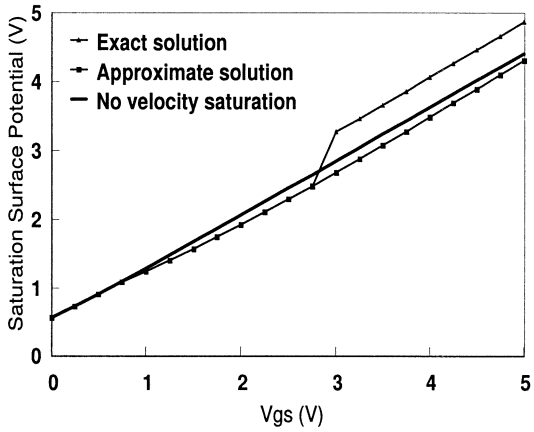

Figure 2: Theoretical profile of ψ_{sLsat} vs. gate voltage, showing a typical numerical discontinuity resulting from using the exact solution of the quartic equation.

Figure 2 gives an example of the improved numerical stability of the approximate solution over the exact quartic solution. It can be seen that the exact solution undergoes a numerical discontinuity around $V_{gs} = 3V$. In addition, beyond this point, it actually exceeds the solution for the case where $S = 1$ (no velocity saturation present). This is a physically impossible result, and illustrates the problems encountered when trying to di-

rectly solve the quartic equation. The range over which such problems occur varies according to the device parameters and operating conditions, but they cannot be solved by standard numerical limiting schemes. By contrast, the approximate solution shows excellent numerical stability even when model parameters are assigned values well outside their physically meaningful ranges.

5 EXPERIMENTAL EVALUATION

The physical nature of the model allows close fitting to experimental data with minimal optimisation of model parameters, as shown in Figures 3 and 4.

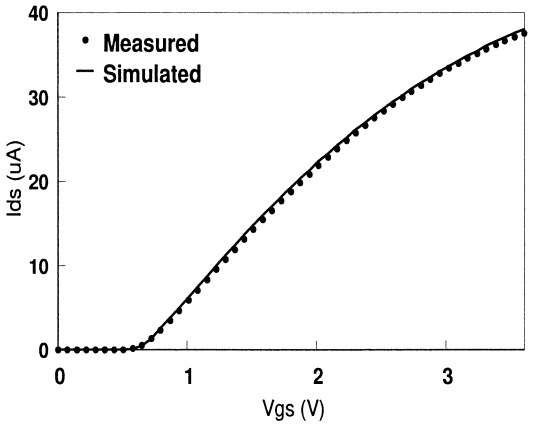

Figure 3: I_{ds} vs. V_{gs} (simulated and measured), for a $50/50\mu m$ body-tied NMOS device ($V_{ds} = 0.1V$).

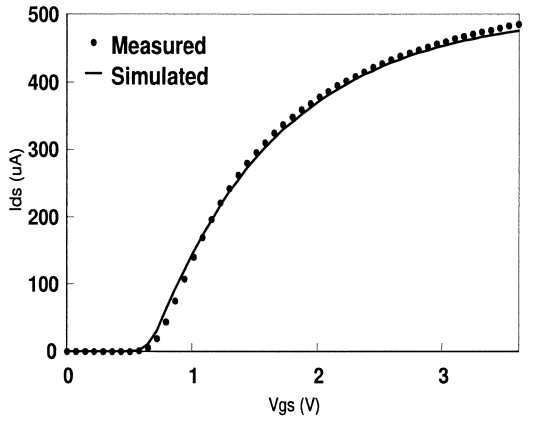

Figure 4: I_{ds} vs. V_{gs} (simulated and measured), for a $10/0.35\mu m$ body-tied NMOS device ($V_{ds} = 0.1V$).

The experimental curves are taken from NMOS devices fabricated in a 0.35μm PD-SOI process. It can be seen that the matching is very good for the $50/50\mu$m device, although it is less ideal for the short-channel $10/0.35\mu$m device. This suggests that there are some shortcomings in the short-channel model, which is not directly related to the vertical mobility model. A single set of mobility parameters was used to simulate the whole range of channel lengths, again underlining the physical nature of the model.

6 CONCLUSION

We have implemented an electron inversion layer mobility model which includes phonon, surface roughness, and Coulomb scattering terms. All terms are retained during calculation of the saturation surface potential, and the resultant quartic solution can be very closely approximated by a stable quadratic solution.

Good matching is achieved using a single parameter set, for a full range of channel lengths. The new model demonstrates a useful technique for ensuring accurate, numerically stable solutions to cubic and quartic expressions. The solution is closed-form, making it suitable for circuit simulation. Although the new mobility model has been tested for PD-SOI MOSFETs, it can be applied with equal validity to bulk devices.

REFERENCES

[1] Y.P. Tsividis, Operation and Modeling of the MOS Transistor, McGraw-Hill Book Company, 1987.

[2] N. Arora, MOSFET Models for VLSI Circuit Simulation, Springer-Verlag, 1993.

[3] C-L. Huang and N.D. Arora, Solid State Electronics, 37, pp 97-103, 1994.

[4] S. Takagi et al., IEEE Transactions of Electron Devices, 41, pp 2357-2362, 1994.

[5] R. van Langevelde and F.M. Klassen, IEEE Transactions of Electron Devices, 44, pp 2044-2052, 1997.

[6] K.Y. Lim and X. Zhou, Solid State Electronics, 45, pp 193-197, 2001.

[7] M.S.L. Lee et al., IEEE Journal of Solid State Circuits, 36, pp 110-121, 2001.

[8] D. Vasileska and D.K. Ferry, IEEE Transactions on Electron Devices, 44, pp 577–583, 1997.

[9] G. Mazzoni et al., IEEE Transactions on Electron Devices, 46, pp 1423–1428, 1999.

[10] S. Villa et al., IEEE Transactions on Electron Devices, 45, pp 110–115, 1998.

[11] A.R. Boothroyd et al., IEEE Transactions on Computer-Aided Design of Integrated Circuits and Systems, 10, pp 1512–1529, 1991.